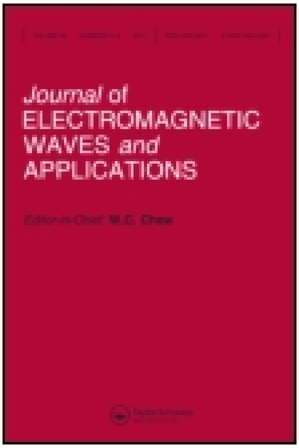


Journal of Electromagnetic Waves and Applications
Publication details, including instructions for authors and subscription information:
http://www.tandfonline.com/loi/tewa20

# Effect of Finite Conductivity On Dispersion Characteristics of Grating Waveguide

C.M. Shiao [a] & S.T. Peng [b]
[a] National Chiao Tung University Department of Communication Engineering Hsinchu, Taiwan, ROC
[b] National Chiao Tung University Department of Communication Engineering Hsinchu, Taiwan, ROC
Published online: 03 Apr 2012.

*Journal of Electromagnetic Waves and Applications*, *Vol. 12, 789–800, 1998*

# EFFECT OF FINITE CONDUCTIVITY ON DISPERSION CHARACTERISTICS OF GRATING WAVEGUIDE

C. M. Shiao and S. T. Peng

National Chiao Tung University
Department of Communication Engineering
Hsinchu, Taiwan, ROC



**Abstract**–We present here a systematic investigation of dielectric waveguide loaded with a metal-strip grating which is realistically characterized by a complex dielectric constant with a negative imaginary part to account for the finite conductivity of the metal strips. The method of mode matching is employed to solve such a boundary-value problem, and the effects of the structure parameters on the dispersion characteristics are critically examined, with a particular attention directed toward the attenuation constant due to the Bragg reflection, radiation and absorption of the grating waveguide.

## 1. INTRODUCTION

We present here a new approach to the analysis of dielectric waveguides loaded with a metal-strip grating. The main objective of this work is to evaluate critically the effect of finite conductivity and non-vanishing thickness of the metal strips on the dispersion characteristics of this class of waveguides. The metal strips are realistically characterized by a complex dielectric constant with a large imaginary part to account for the finite conductivity, so that the metal-strip grating may be treated as a dielectric one in which the electromagnetic fields everywhere can be determined. Thus, the effect of the finite conductivity can be explored to the full extent.

In the literature, grating waveguides have been a subject of continuing interest for their various applications, such as the design of the input/output couplers and beam splitters for optical applications, and leaky wave antennas and polarization converters for microwave and millimeter-wave applications [1–3]. This class of structures offers many advantages, such as: the beam steering capability by frequency variation, the ease of flush-mount to form integrated-circuit systems. The strip-loaded structure has been a subject of experimental and theoretical studies [5–14]; in the past, the theoretical analysis had been mostly restricted to small-obstacle or small-aperture approximation, corresponding to the width of metal strips much smaller or much larger than that of the air grooves [5–7]. Nevertheless, they had laid a theoretical foundation for the analysis of dispersion characteristics of grating waveguides. Subsequently, many rigorous methods have been introduced, such as: the spectral domain method [10, 11], the method of multimode transverse equivalent network [12], the method of mode matching [13], and the method of boundary-integral-equation [14]; however, they are limited by the assumption of perfectly conducting metal strips, often with infinitesimal thickness.

The grating waveguide under consideration is a multilayer structure which is assumed to be infinite in extent. For simplicity, we restrict ourselves to the special case where the guiding direction is assumed to be normal to the metal strips. For such a two-dimensional boundary-value problem, we employ the method of mode matching to treat rigorously the TE- and TM-modes guided by the structure [1]. A unique feature of our analysis is to divide the Floquet modes into two subsets: air modes and metal modes [15, 16]. Specifically, the modes supported by the air spacing between two neighboring metal strips are the "perturbed parallel-plate waveguide modes" due to the finite conductivity of the metal strips, and they will be referred to as the air modes for simplicity. In addition, there exists another set of modes residing inside the metal strips, which are called the metal modes, and it takes the two subsets together to form a judicial representation for the fields inside the grating layer. It had been shown [16] that the air modes are responsible for the edge-current distribution, while the metal modes are responsible for the surface-current distribution. With such a new approach, we have carried out numerical simulations to demonstrate the effects of the conductivity and thickness of the grating on the dispersion characteristics in terms of $k_o$-$\beta$ and $k_o$-$\alpha$ diagrams, including the separate evaluations of the attenuation constant due to the Bragg phenomenon, the energy leakage, and power dissipation within the lossy metal. In this way, a physical picture of the loss mechanism within the structure is clearly established, and suggestions are made to take advantage of these parameters for the design of grating waveguides.

## 2. FORMULATION

Figure 1 shows the geometry of the waveguide structure under consideration, together with the coordinate system indicated. It consists of a guiding film supported by a large substrate and is loaded with a metal grating. The

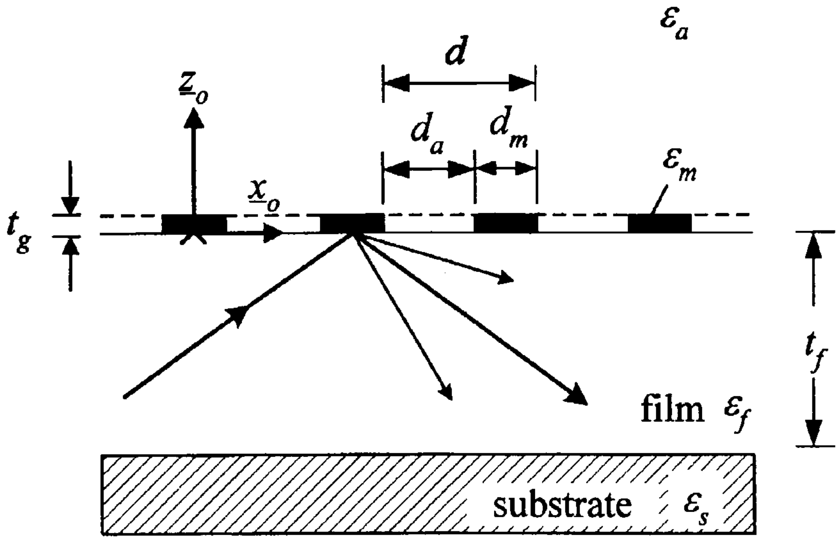


**Figure 1.** Geometry of metal grating waveguide.



guiding film has a dielectric constant $\varepsilon_f$, and a thickness $t_f$. The grating is composed of metal strips that are periodically deposited with a period $d$ and a finite thickness $t_g$. The spacings between two neighboring metal strips of the grating are filled with air, and will be refereed to as the air grooves. The upper half space covering the grating is assumed to be air, with the dielectric constant $\varepsilon_a$. The substrate is semi-infinite in extent, with the dielectric constant $\varepsilon_s$. In the present analysis, every dielectric constant may be taken as a complex quantity with an imaginary part to account for the absorption effect of the medium. In particular, a metal of finite conductivity $\sigma$ may be characterized by a complex dielectric constant with a large imaginary part, as:

$$\varepsilon_m = 1 - j60\sigma\lambda \tag{1}$$

where $\lambda$ is the operating wavelength. It is noted that the negative sign in the last equation reflects the fact that the time dependence of the form $e^{j\omega t}$ has been assumed and suppressed. Furthermore, the dielectric substrate may be replaced by a ground plane, with a complex dielectric constant, as described above. In this way, the structure under consideration may be regarded as a dielectric one which had been extensively investigated in the literature [1].

Following the formulation previously developed [17], the tangential field components with respect to the $z$-direction may be denoted by: $E(x, z) =$

$E_y(x,z)$ and $H(x,z) = H_x(x,z)$ for TE mode, and $E(x,z) = E_x(x,z)$ and $H(x,z) = H_y(x,z)$ for TM mode. These field components in the grating region may be represented in the form:

$$E(x,z) = \sum_{i=-\infty}^{\infty} F_i(x)V_i(z) \tag{2}$$

$$H(x,z) = \sum_{i=-\infty}^{\infty} F_i(x)I_i(z) \tag{3}$$

where $F_i(x)$ is the $i^{\text{th}}$ Floquet mode function of the grating and can be expressed in terms of the Fourier series, as:

$$F_i(x) = \sum_{n=-\infty}^{\infty} P_n^{(i)} e^{-j\kappa_n x} \tag{4}$$

with

$$\kappa_n = \kappa + \frac{2n\pi}{d} \tag{5}$$

For the guiding problem under consideration, $\kappa$ is the propagation constant in the $x$-direction to be determined from the boundary-value problem of the grating waveguide, while $\kappa_n$ is related to $\kappa$ for every integer $n$. For a given value of $\kappa$, a set of the space harmonics, $P_n^{(i)}$, can readily be determined. Furthermore, $V_i(z)$ and $I_i(z)$ stand for the vertical variations of the tangential electric and magnetic fields, respectively, and they satisfy the transmission line equations:

$$\frac{d}{dz}V_i(z) = -jk_{zi}Z_iI_i(z) \tag{6}$$

$$\frac{d}{dz}I_i(z) = -jk_{zi}Y_iV_i(z) \tag{7}$$

where $k_{zi}$ is the transverse propagation constant (in the $z$-direction) of the $i^{\text{th}}$ mode, and $Z_i$ and $Y_i$ are the impedance and admittance of the transmission line. These transmission-line parameters are determined through the dispersion relation [17]:

$$\cos\kappa d = \cos\kappa_a d_a \cos\kappa_m d_m - \frac{1}{2}\left(\frac{Z_a}{Z_m} + \frac{Z_m}{Z_a}\right)\sin\kappa_a d_a \sin\kappa_m d_m \tag{8}$$

with the

$$\kappa_a = \sqrt{k_o^2\varepsilon_a - k_{zi}^2} \tag{9}$$

$$Z_a = \begin{cases} \dfrac{\omega\mu_o}{\kappa_a}, & \text{for TE modes} \\ \dfrac{\kappa_a}{\omega\varepsilon_o\varepsilon_a}, & \text{for TM modes} \end{cases} \tag{10}$$

for the air region, and similarly for the set with the subscript $a$ replaced by $m$ for the metal region. Evidently, the dispersion relation is a transcendental equation to determine the transverse propagation constant $k_{zi}$, for $a$ given $\kappa$. Thus, the electromagnetic fields in the grating region are completely determined.

Outside the grating region, we have all uniform media where every space harmonic is a plane wave, regardless of its polarization. The complex amplitudes of space harmonics in each region are determined by the method of mode matching, that is, requiring the continuity of the tangential field components across the interfaces at $z = t_g$, 0, and $-t_f$. This results in a set of homogeneous system of linear equations, for which the condition for the existence of a nontrivial solution leads to the dispersion relation in the form of an infinite determinant to determine the complex propagation constant $\kappa = \beta - j\alpha$ for the grating waveguide [17].



## 3. NUMERICAL RESULTS

For the numerical analysis to follow, we shall choose copper for the metal strips, with the conductivity $\sigma = 5.8 \times 10^4$ S/mm, unless otherwise specified. Furthermore, the infinite systems of linear equations for the space harmonics have to be truncated to finite ones for an approximate analysis; in most cases, 60 space harmonics are included. It is noted that analogous to the relative convergence in the case of bifurcated waveguide, the ratio between the numbers of air and metal modes must be about the same as the ratio between the widths of air spacings and the metal strips.

To check the accuracy of the present method, we compare our results to those obtained by the numerical boundary-integral-equation method [14] for thick strip grating structure with the assumption of perfect conductor. Fig. 2 shows the dependence of the propagation and decay constants on the grating thickness by the two methods, for both TE- and TM- polarization. Evidently the results of the two methods agree quite well with each other, particularly for the case of TE polarization. Physically, for the structure parameters chosen, all air modes are below cutoff, except for the TEM mode; thus, the phase and decay constants tend monotonically to a limit for the TE case, but not for the TM case, as expected.

Figure 3 shows the Brillouin diagram for a dielectric waveguide loaded with metal grating, for the case of TM-polarization. The dispersion characteristics are expressed in terms of the $k_o$-$\beta$ and $k_o$-$\alpha$ diagrams. The guiding film has the dielectric constant $\varepsilon_f = 12$ and thickness $t_f = 0.22$ mm. The metal grating has an very small thickness $t_g = 0.001$ mm., while the widths of air spacing and metal strip are: $d_a = d_m = 0.2$ mm. Also shown are the

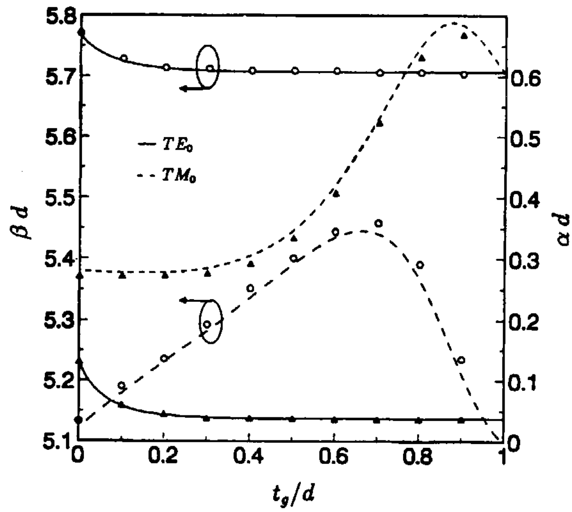


**Figure 2.** Comparison between the results of mode matching method and that of Ref. [14]. The structure parameters are: $d_a = d_m = 1$ mm, $t_f = 1$ mm, $k_0 d = 2.1, \varepsilon_f = 11.8$, and $\varepsilon_s = 1$.

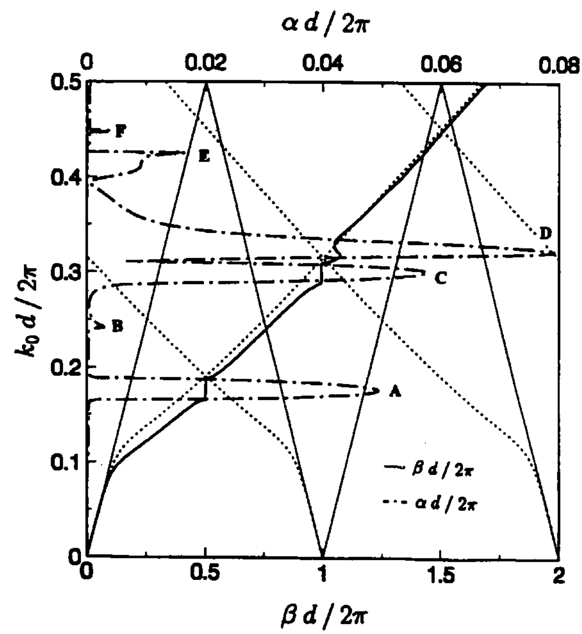


**Figure 3.** The Brillouin diagram for metal grating waveguide. The structure parameters are: $d_a = d_m = 0.2$ mm, $t_f = 0.22$ mm, $t_g = 10^{-3}$ mm, and $\varepsilon_f = 12$.

unperturbed dispersion curves for the structure in the absence of the grating and the bound- wave triangles, in the dotted and thin solid lines, respectively. It is observed that the real part of the dispersion curve varies only slightly from the unperturbed one, except in some small frequency ranges, to be elaborated below.

The Brillouin diagram is divided by the bound-wave triangle into two types of region, the slow-wave or bound-wave region and the fast-wave or leaky-wave region. For a lossless periodic structure, the propagation constant of a slow wave is purely real in the passband and complex with a fixed real part in the stop band [4–12]. In contrast, our analysis includes the finite conductivity of the metal, so that the structure is now lossy and the propagation constant is generally complex at any frequency, with the real part for the phase constant and the imaginary part for the attenuation constant. Evidently, the attenuation constant is rather small, except in some frequency ranges where spikes occur, as labeled by A, B, C, and so on. The spike A represents the first stopband with the peak at around $k_od/2\pi = 0.17$. Since the first stopband is in the bound-wave region, the real part of the propagation constant has roughly the value: $\beta d/2\pi = 0.5$. As the frequency is increased, the guided wave enters into the fast-wave region at about $k_od/2\pi = 0.24$, with the radiation direction starting in backward endfire direction. Here, the spike B corresponds to the on-set of such a backward endfire radiation. By increasing the frequency further, the radiation direction sweeps from the backward endfire to the broadside direction; in the small range of frequency around the value $k_od/2\pi = 0.3$, we have another spike labeled by C, which corresponds to the second stopband where $\beta d/2\pi = 1$. With the frequency further increased slightly, the forward radiation begins at around the frequency $k_od/2\pi = 0.31$ and ends at the frequency around $k_od/2\pi = 0.425$. In this frequency range, we have two spikes labeled by D and E; the former is the largest and represents the strongest radiation, while the latter corresponds to the forward endfire radiation. Finally, spike F represent the third stopband. An overall feature of this structure is that the backward radiation is rather weak, as the decay constant remains quite small over its entire range of operation; on the other hand, the forward radiation appears very strong, particularly near the broadside direction, as exemplified by the spike labeled by D. To see the effect of the film thickness, Fig. 4 shows the Brillouin diagram for the case $t_f = 0.27$ mm. The general behaviors of the curves stay the same as those in Fig. 3, except that the radiation is strong in the backward but not the forward direction.

Fig. 5 shows the Brillouin diagram for a case of narrow metal strips, corresponding to a perturbation of small obstacles, for three different values of the

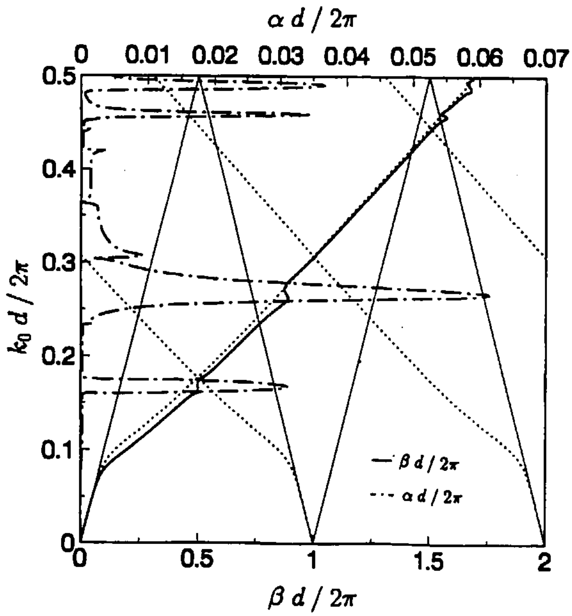


**Figure 4.** The Brillouin diagram for metal grating waveguide. The parameters are the same as Fig. 3 except $t_f = 0.27$ mm.

conductivity. It is noted that the phase constant follows closely the unperturbed line, as expected for a small perturbation to the dielectric waveguide. Looking at the solid curve for the case of good conductor ($\sigma = 5.8 \times 10^4$ S/mm), the ohmic loss is small and the attenuation constant is attributed mainly to the radiation or the stopband behavior. Comparing the curves for the phase constant, we observe that the stopbands are not appreciably affected by the value of the conductivity. On the other hand, outside the stopbands, the attenuation-constant curves for three different values of conductivity deviate from one another substantially; for the frequency range investigated, the normalized attenuation constant, $\alpha d/2\pi$, is increased by about $4 \times 10^{-3}$ for every decade of decreasing conductivity. Furthermore, by inspection of each attenuation curve, the portion in the bound-wave region is mainly due to the ground plane, while the jump at around $k_o d/2\pi = 0.29$ is obviously due to the radiation effect. Again, comparing the three attenuation curves, we may assert that the radiation characteristics of the the leaky-wave antenna is not affected appreciably by the conductivity of the metal.

While the effect of the grating thickness on the guiding characteristics is shown in Fig. 2 at a single frequency, Fig. 6 demonstrates the effect over

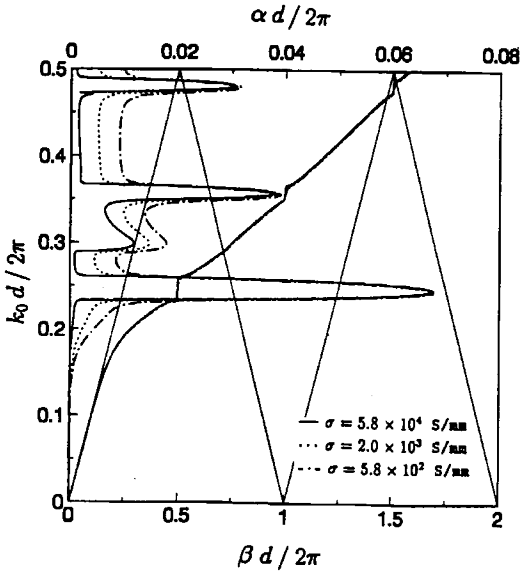


**Figure 5.** The effect of finite conductivity on the dispersion characteristics of narrow metal-strip grating waveguide. The structure parameters are: $d_a = 0.3$ mm, $d_m = 0.1$ mm, $t_f = 0.12$ mm, $t_g = 10^{-3}$ mm, and $\varepsilon_f = 12$.

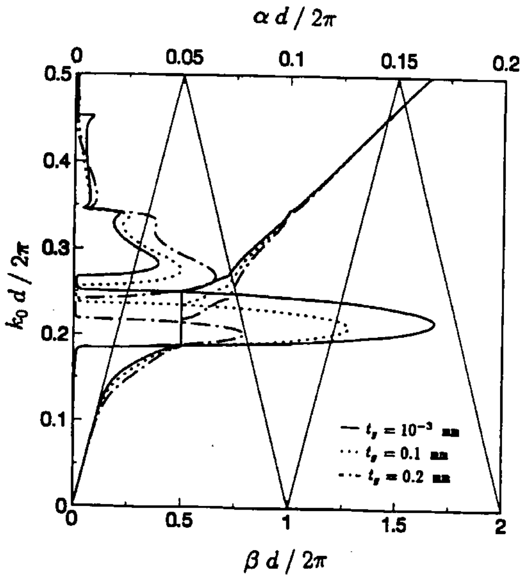


**Figure 6.** The effect of finite strip thickness on the dispersion characteristics of metal strip grating waveguide. The structure parameters are: $t_f = 0.12$ mm, $d_a = d_m = 0.2$ mm, and $\varepsilon_f = 12$.

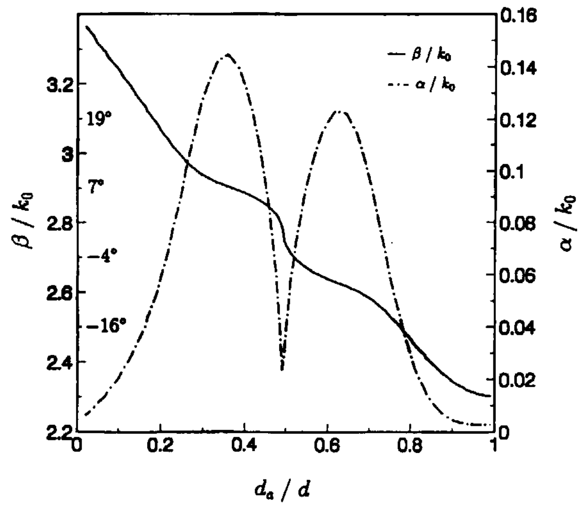


**Figure 7.** The effect of aspect ratio of metal grating on the propagation and leakage constant. The second ordinate inside the plot is the corresponding angle of radiation. The structure parameters are: $d = 0.4$ mm, $\lambda = 1.11$ mm, $t_f = 0.1$ mm, $t_g = 10^{-3}$ mm, and $\varepsilon_f = 12$.

a frequency band of practical interest for the fundamental TM mode of a structure with the parameters indicated. It is interesting to observe in this case of low loss structure that as the thickness is increased, the stopband is reduced but the backward radiation is increased. Evidently, the grating thickness is an important factor to consider for both filter and antenna designs.

Fig. 7 shows the dependence of the normalized phase and leakage constant, $\beta/k_o$ and $\alpha/k_o$, on the variation of grating aspect ratio, $d_a/d$. Also indicated on the vertical axis are the radiation angles. For the frequency chosen, $\lambda = 1.11$ mm, the main radiating beam sweeps through the broadside direction, as the aspect ratio is changed. Since the leakage constant vanishes at the broadside radiation, the attenuation shows the dip at $d_a/d = 0.5$. This means physically that the aspect ratio may affect the phase constant of the waveguide and cause the drastic change in the radiation characteristics.

## 4. CONCLUSION

The dispersion characteristics of dielectric waveguides loaded with a metal-strip grating are analyzed by the method of mode matching. Within the metal-strip grating, the complete set of the Floquet modes are divided into two subsets of air modes and metal modes, so that the electromagnetic fields are represented judicially in terms of the two subsets. This approach permits the evaluation of the attenuation constant separately due to the Bragg reflection, the leakage of energy, and power dissipation in the lossy metal. The dispersion characteristics of the grating waveguide is displayed in the form of $k_o$-$\beta$ and $k_o$-$\alpha$ diagrams. It is shown that the finite conductivity and non-vanishing thickness of the metal strips have profound effects on the dispersion behavior of the guided waves and may be used to advantage for the design of leaky-wave antennas and band-reject filters using this type of structures.



## ACKNOWLEDGEMENT

This research was supported by the National Science Council of the Republic of China, under the contract No. NSC87-2213-E009-125.

## REFERENCES

1. Schwering, F., and S. T. Peng, "Design of dielectric grating antennas for millimeter-wave applications," *IEEE Trans. MTT,* Vol. MTT-31, 199–209, Feb. 1983, and the references therein.
2. Itoh, T., "Application of grating in dielectric wavegide for leaky-wave antennas and band-reject filters," *IEEE Trans. MTT,* Vol. MTT-25, No. 12, 1134–1137, Dec. 1977.
3. Peng, S. T., M. J. Shiau, A. A. Oliner, J. Borowick, W. Bayha, and F. Schwering, "A simple analysis procedure for dielectric grating antennas of finite width," *IEEE AP-S Int. Symp.,* Boston, MA., June 1984.
4. Collin, R. E., and F. J. Zucker, Eds., *Antenna Theory,* Chap.19, Part 2, McGraw-Hill, New York, 1969.
5. Jacobsen, J., "Analytical, numerical, and experimental investigation of guided waves on a periodically strip-loaded dielectric slab," *IEEE Trans. Antenna Propagat.* Vol. AP-18, No. 3, 379–388, May 1970.
6. Sigelmann, R. A., "Surface waves on a grounded dielectric slab covered by a periodically slotted conducting plane," *IEEE Trans. Antenna Propagat.,* Vol. AP-15, 672–676, Sept. 1967.
7. Balling, P., "Periodically modulated dielectrically filled waveguide as a microwave antenna, *Electronic Lett.,* Vol. 5, 508–510, Oct. 1969.
8. Kobayashi, S., R. Lampe, R. Mittra, and S. Ray, "Dielectric rod leaky-wave antennas for millimeter-wave applications," *IEEE Trans. Antenna Propagat.,* Vol. AP-29, No. 5, 822–824, Sept. 1981.

9. Trinh, T. N., R. Mittra, and R. J. Paleta, Jr., "Horn image guide leaky wave antenna," *IEEE Trans. MTT,* Vol. MTT-29, No. 12,1310–1314, Dec. 1981.
10. Mittra, R., and R. Kastner, "A Spectral domain approach for computing the radiation characteristics of leaky-wave antennas for millimeter waves," *IEEE Trans. Antenna Propagat.,* Vol. AP-28, 652–654, July 1981.
11. Ogusu, K., "Propagation properties of a planar dielectric waveguide with periodic Metallic Strips," *IEEE Trans. MTT,* Vol. MTT-29, No. 1, 16–21, Jan. 1981.
12. Guglielmi, M., and A. A. Oliner, "A practical theory for dielectric image guide leaky-wave antenna loaded by periodic metal strips, *17th European Microwave Conf. Proc.,* 549–554, Sept. 1987.
13. Encinar, J. A., "Mode-matching and point matching techniques applied to the analysis of metal strip-loaded dielectric antennas," *IEEE Trans. Antenna Propagat.,* Vol. AP-38, No. 9, 1405–1412, Sept. 1990.
14. Matsumoto, M., M. Tsutsumi, and N. Kumagai, "Radiation characteristics of a dielectric slab waveguide periodically loaded with thick metal strips," *IEEE Trans. MTT,* Vol. MTT-35, No. 2, 89–95, Feb. 1987.
15. Peng, S. T., and C. M. Shiao, "Wave scattering by metallic strip grating," *IEEE MTT International Microwave Symposium, San Diego,* 879–882, May 223-26, 1994.
16. Shiao, C. M., and S. T. Peng, "Edge current on metal-strip gratings," Accepted for Presentation, *IEEE AP-S/URSI Symposium,* 1997.
17. Peng, S. T., and T. Tamir, and H. L. Bertoni, "Theory of periodic dielectric waveguides," *IEEE Trans. MTT,* Vol. MTT-23, 123–133, Jan. 1975.

**S. T. Peng** is a Professor of Communication Engineering and is currently serving as the Director of Center for Telecommunications Research at the National Chiao Tung University, Taiwan, Republic of China. He has been active in various IEEE activites and is serving as the founding Chairman of the Taipei Chapter, IEEE EMC Society. For his professional contributions, he was elected a fellow of IEEE, SPIE and the Academy of Electromagnetics.

**Chi-Ming Shiao** received his B.E. and M.S. degrees from the National Chiao Tung University, Hsinchu, Taiwan, in 1990 and 1992, respectively. He is currently pursuing the Ph.D. degree in communication engineering at the same school. His research interests include the analysis of scattering and guiding characteristics of periodic structures and RF circuits design for wireless communications.